Toward the Rational Design of Superoxide Dismutase Mimics: Mechanistic Studies for the Elucidation of Substituent Effects on the Catalytic Activity of Macrocyclic Manganese(II) Complexes

Dennis P. Riley,* Patrick J. Lennon, William L. Neumann, and Randy H. Weiss

Contribution from the The Monsanto Company, 800 North Lindbergh Boulevard, St. Louis, Missouri 63167

Abstract: Two new isomeric bis(*trans*-fused cyclohexano) substituted 1,4,7,10,13-pentaazacyclopentadecane ligands and their Mn(II) complexes, **3** and **4**, have been synthesized, and their activity as superoxide dismutase (SOD) catalysts has been studied. Complex **3** is an excellent SOD catalyst with a second-order rate constant at pH = 7.4 of $1.2 \times 10^{+8}$ M^{-1} s^{-1}. In contrast, the isomeric complex **4** has virtually no detectable catalytic SOD activity, implying the need to understand the effect that the position, number, and stereochemistry of substituents exert on the catalytic rate. The crystal structure of the complex **4** was determined and reveals that the Mn(II) ion is coordinated in a pentagonal bipyramid array of the five nitrogens of the macrocyclic ligand and capped by two *trans*-chloro ligands. Crystal data for $MnC_{18}H_{37}Cl_2N_5$ are as follows: triclinic at 20 °C, space group P_1--C_i2 (no. 2); $a = 9.746(3)$ Å, $b = 12.631(6)$ Å, $c = 11.311(5)$ Å; $\alpha = 73.14(4)°$, $\beta = 76.39(3)°$, $\gamma = 79.98(3)°$, V = 1287(1) Å³, and Z = 2 ($\rho_{calc} = 1.279$ g/cm³; μ_a Mo $K_\alpha = 6.23$ mm⁻¹). Mechanistic studies with the complex **3** and the pentamethyl susbstituted complex, **5**, including D_2O rate studies, are reported and are consistent with the existence of two pathways for the rate-determining electron-transfer from Mn(II) to superoxide: (1) hydrogen atom transfer from a bound water on Mn(II) to $HO_2^\bullet$ to yield a Mn(III) hydroxo intermediate and (2) the dissociative pathway in which superoxide anion binds to a vacant coordination site on Mn(II) followed by protonation/oxidation to yield a Mn(III)hydroperoxo species. Subsequent reduction of the intermediate Mn(III) with superoxide anion completes the catalytic cycle. Substituent effects on the rates and relative contribution of the two pathways to the overall rate of SOD activity is ascribed to the propensity of the ligand to fold around Mn(II) forming a pseudo-octahedral complex similar in geometry to the oxidized Mn(III) complex. Folding of the pentaaza macrocyclic ligand is confirmed as a relevant structural motif for this series of Mn(II) complexes by the X-ray structure determination of the bis(nitrate) derivative of **1**, [Mn-$(C_{10}H_{25}N_5)NO_3]NO_3$, which reveals a six-coordinate structure with a folded conformation of the macrocyclic ligand. Crystal data for [Mn($C_{10}H_{25}N_5$)NO₃]NO₃: orthorhombic at −100 °C, space group $P2_12_12_1$; $a = 9.457(2)$ Å, $b = 12.758(2)$ Å, $c = 13.834(2)$ Å, V = 1669.1(5) Å³, and Z = 4 ($\rho_{calc} = 1.549$ g/cm³).

Introduction

We have shown that the pentaaza macrocyclic Mn(II) complex, **1** (Figure 1),[1] and derivatives of this complex which bear substituents on the carbon atoms of the macrocycle[2] are highly active and stable superoxide dismutase (SOD) mimics. In numerous biological studies both *in vitro* and *in vivo* these complexes display potent mechanism-based biological effects.[3] Our goal has been to design low molecular weight, nonpeptidic molecules possessing the function of human enzymes but eliminating some of the negatives associated with the use of peptide-based pharmaceuticals; e.g., cost, immunogenicity, tissue penetration, oral bioavailability, etc. Successful implementation of such metal-based drugs as human pharmaceutical agents mandates that we construct molecules with high inherent chemical stability while retaining high SOD activity. Recently,[2] we reported that increasing the number of substituents on the carbon atoms of the macrocycle invariably increases stability (both kinetic and thermodynamic) of the Mn(II) complexes derived from **1**. Additionally, we observed that the number, position, and stereochemistry of the substituents on the carbon
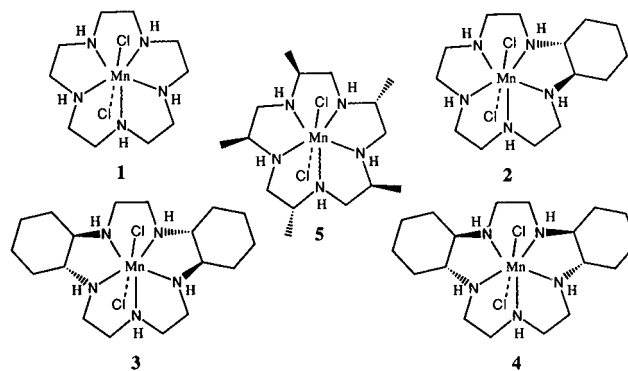

Figure 1. Mn(II) dichloro complexes of the carbon substituted pentaaza macrocyclic ligands utilized in this study.

atoms of the macrocyclic ring exert a dramatic effect on the catalytic SOD activity of the resultant complex.

In order to focus our synthetic efforts on the rational construction of both highly stable (maximize substituents) and highly SOD active Mn(II) complexes, we have studied the superoxide dismutase catalytic reaction mechanism in detail. This understanding is absolutely essential for the rational design of these SOD catalysts as we have observed that the two effects do not necessarily work in concert; i.e., simply increasing the number of substituents does not guarantee that the resultant Mn(II) complex will possess any SOD activity. Herein, we

⊗ Abstract published in *Advance ACS Abstracts,* June 15, 1997.
(1) Riley, D. P.; Weiss, R. H. *J. Am. Chem. Soc.,* **1994,** *116*, 387.
(2) Riley, D. P.; Henke, S. L.; Lennon, P. J.; Weiss, R. H.; Neumann, W. L., Rivers Jr, W. J.; Aston, K. W.; Sample, K. R.; Rahman, H.; Ling, C,-S.; Shieh, J.-J.; Busch, D. H.; Szulbinski, W. *Inorg. Chem.* **1996,** *35*, 5213.

Superoxide Dismutase Mimics

J. Am. Chem. Soc., Vol. 119, No. 28, 1997 6523

report our efforts to understand the details of the electron-transfer process and describe two new complexes incorporating two *trans*-fused cyclohexano backbones on the macrocyclic ring ligands[4] — a structural motif which enhances both the stability and activity; e.g., complex **2**, which possesses one *trans*-cyclohexano substituent is more than twice as active as **1** as a SOD catalyst and is both kinetically (2-fold enhancement) and thermodynamically (log $K = 11.6$ vs 10.8 for **1**) more stable than the parent unsubstituted complex, **1**.

We also report here the X-ray crystal structure of two new complexes. One of the new complexes is the bis(*trans*)-cyclohexano derivatives, **4**, which crystallized as the seven-coordinate dichloro derivative. The second complex is the bis(nitrato) derivative of complex **1**, which was crystallized as the six-coordinate nitrato nitrate complex. The relevance of this new six-coordinate nitrato derivative to these studies will be discussed.

Experimental Section

Syntheses of Ligands: *N*,*N*′-Bis(chloroacetyl)-1*R*,2*R*-diaminocyclohexane. 1*R*,2*R*-(−)-Diaminocyclohexane (6.98 g, 61.11 mmol) was dissolved in 75 mL of alcohol free CHCl₃ in a four-neck, 2000 mL round bottom flask along with 37 mL of H₂O under argon. Two Normag dropping funnels were connected to the reaction flask and charged separately with chloroacetyl chloride (15 mL, 188.3 mmol) in alcohol free CHCl₃ (88 mL) and K₂CO₃ (24.1 g, 174.4 mmol) in 918 mL of H₂O. An internal thermometer was inserted into the reaction flask. After cooling the two phase mixture in the reaction flask to 0 °C in an ice bath, the additions from the dropping funnels were started in such a way as to keep the proportion of each solution added approximately equal over a 1 h 20 min period. During the addition, an ice salt bath was used to moderate the temperature, keeping it between 3 and −3 °C. A shell of ice formed on the inside of the reaction flask which did not seem to impede the stirring. The reaction flask was removed from the ice bath at the end of the addition and was stirred for 2 h 20 min. The lower chloroform layer appeared to have a considerable quantity of a light solid in it at ice bath temperature, but it dissolved as the reaction warmed. The reaction mixture was placed in a separatory funnel, some additional chloroform added, and the layers were separated. The aqueous layer was extracted with another portion of CHCl₃, and the combined chloroform layers were washed with water, then saturated NaCl, dried (Na₂SO₄), and stripped down to a brownish white solid. This solid was stirred overnight with about 450 mL of ether and then filtered, much of the color staying in the ether, giving a beige solid, 13.68 g, 51.60 mmol, 84.4% yield. ¹H NMR (CDCl₃, 400 MHz) δ 1.34 (m, 4H), 1.80 (m, 2H), 2.08 (m, 2H), 3.74 (m, 2H), 3.99 (ABq, $J = 15.1$ Hz, $\delta\nu = 8.2$ Hz, 4H), 6.78 (br s, 2H); ¹³C NMR (CDCl₃, 100 MHz) δ 24.59, 32.07, 42.45, 53.94, 166.65; MS (FAB, NBA-LiCl matrix): *m/z* (rel intensity) 273 (100) [M + Li]⁺, 275 (71) [M + Li]⁺.

(3) a) Weiss, R. H.; Flickinger, A. G.; Rivers, W. J.; Hardy, M. M.; Aston, K. W.; Ryan, U. S.; Riley, D. P. *J. Biol. Chem.* **1993**, *268*, 23049−23054. (b) Weiss, R. H.; Riley, D. P.; Rivers, W. J.; Aston, K. W.; Flickinger, A. G.; Hardy, M. M.; Ryan, U. S. Manganese-Based Superoxide Dismutase Mimics: Design, Discovery and Pharmacologic Efficacies In *The Oxygen Paradox*; Davies, K. J. A., Ursini, F., Eds.; CLEUP University Press: Padova, Italy, 1995; pp 641−651. (c) Weiss, R. H.; Fretland, D. J.; Baron, D. A.; Ryan, U. S.; Riley, D. P. *J. Biol. Chem.* 1996, *271*, 26149. (d) Kasten, T. P.; Settle, S. L.; Misko, T. P.; Riley, D. P.; Weiss, R. H.; Currie, M. G.; Nickols, G. A. *Proc. Soc. Exp. Biol. Med.* **1995**, *208*, 170−177. (e) Hardy, M. M.; Flickinger, A. G.; Riley, D. P.; Weiss, R. H.; Ryan, U. S. *J. Biol. Chem.* **1994**, *269*, 18535−18540. (f) Kilgore, K. S.; Friedrichs, G. S.; Johnson, C. R.; Schasteen, C. S.; Weiss; R. H.; Riley, D. P.; Ryan, U. S.; Lucchesi, B. R. *J. Mol. Cell. Cardiol.* **1994**, *26*, 995−1006. (g) Black, S. C.; Schasteen, C. S.; Weiss, R. H.; Riley, D. P.; Driscoll, E. M.; Lucchesi, B. R. *J. Pharmacol. Exp. Therapeut.* **1994**, *270*, 1208−1215. (h) Venturini, C. M.; Sawyer, W. B.; Smith, M. E.; Palomo, M. A.; McMahon, E. G.; Weiss R. H.; Riley, D. P.; Schasteen, C. S. In *The Biology of Nitric Oxide*; Moncada, S., Feelisch, M., Busse, R., Higgs, E. A., Eds.; Portland Press: London, 1994; Vol. 3, pp 65−9.

(4) (a) Lennon, P. J.; Rahman, H.; Aston, K. W.; Henke, S. L.; Riley, D. P. *Tetrahedron Lett.* **1994**, *35*, 853. (b) Neumann, W. L.; Franklin, G. N.; Sample, K. R.; Riley, D. P.; Rath, N. *Tetrahedron Lett.* **1997**, *38*, 3143.

N-Tosylglycyl-(1*R*,2*R*)-diaminocyclohexane. (1*R*,2*R*)-Diaminocyclohexane (10.0 g, 87.57 mmol) was dissolved in dry DMF (150 mL) under argon and cooled to −10 °C. Separately, *N*-tosylglycine (10.04 g, 43.62 mmol), 1-hydroxybenzotriazole (6.75 g, 44.08 mmol), and 1-ethyl-3-(3-dimethylaminopropyl)carbodiimide hydrochloride (8.45 g, 44.05 mmol) were dissolved in dry DMF (150 mL) and cooled to −10 °C under argon. The latter solution was added to the diaminocyclohexane solution at −10 °C via cannula. After 2 h at this temperature, water (8 mL) was added and the reaction was allowed to warm to 0 °C over 1 h and then to room temperature over the next half hour. The solvent was removed on the rotary evaporator under reduced pressure. The residue was heated to 40−42 °C with water (150 mL) added in small portions with stirring. After 25 min this solution was filtered. The white precipitate was largely the bis adduct (5.55 g). Exactly 68 mL of the filtrate was worked up by repeated extraction with dichloromethane (9 × 50 mL). The combined organic phase was dried (sodium sulfate) and filtered, and the solvent was removed. The resulting white solid which contained some residual DMF was redissolved in dichloromethane (30 mL) and added dropwise to a stirred solution of 9:1 ether:hexane (250−300 mL) giving an immediate precipitate which was stirred overnight and then filtered. This procedure was repeated, stirring for 3 h instead of overnight. After drying the white product on the vacuum line, 2.36 g, 7.25 mmol were obtained, equivalent to a 36.7% yield for the entire reaction. ¹H NMR (CDCl₃, 400 MHz) δ 1.10−1.34 (m, 4H), 1.70 (d, $J = 9.7$ Hz, 2H), 1.81−1.97 (2 m, 2H), 2.41 (s, 3H), 2.51 (td, $J = 10.2, 3.8$ Hz, 1H), 3.53 (m + ABq, $J = 16.9$ Hz, $\delta\nu = 51.6$ Hz, 3H), 3.69 (br s, 3H), 6.84 (d, $J = 9.1$ Hz, 1H), 7.30 (d, $J = 8.3$ Hz, 2H), 7.73 (d, $J = 8.3$ Hz, 2H); ¹³C NMR (CDCl₃, 100 MHz) δ 21.48, 24.87, 24.97, 32.08, 35.16, 46.09, 54.85, 55.78, 127.15, 129.85, 136.02, 143.84, 168.69; MS (GT HCl): *m/z* 326 (100) [M + H]⁺.

(2*R*,3*R*,8*R*,9*R*)-Dicyclohexano-13-*p*-toluenesulfonyl-1,4,7,10,13-pentaazacyclopentadecan-5,11,15-trione. *N*-*p*-Toluenesulfonylglycyl-(1*R*,2*R*)-diaminocyclohexane (1.11 g, 3.42 mmol) and *N*,*N*′-bis-(chloroacetyl)-(1*R*,2*R*)-diaminocyclohexane (0.913 g, 3.42 mmol) were combined in a 1-L flask and dry *N*,*N*-dimethylacetamide (650 mL) was added. The flask was inerted. After 10 min, the sodium hydride (0.19 g, 95%) was added directly to the homogeneous mixture. The reaction flask was placed in a 70 °C oil bath. After the internal temperature reached 45−50 °C, gas evolution became constant. The oil bath temperature was stabilized at about 65 °C with some excursions from about 60 to 75 °C. Overnight, the reaction mixture became homogeneous. After heating for 17 h the reaction flask was removed from the bath and allowed to cool. The solvent was removed under reduced pressure, and the yellowish oil was placed on the vacuum line. The residue was treated with dichloromethane (300 mL) and washed with water (40 mL) and twice with saturated sodium chloride (40 mL each). After combining, the aqueous layers were backwashed with dichloromethane (100 mL). The combined organic layers were dried over sodium sulfate, filtered, and stripped down to a viscous yellow oil which was placed on the vacuum line, 2.14 g. This residue was chromatographed using 0.5% NH₄OH/9% CH₃OH/90.5% CH₂Cl₂. On TLC on silica using the same system, $R_f = 0.25$. Fractions containing the correct spot were combined and evaporated down to a slightly off white solid, 0.89 g, 1.71 mmol, 50.1% yield. ¹H NMR (CDCl₃, 300 MHz) δ 0.92−2.1 (several m, 16H), 2.27 (m, 1H), 2.41 (s, 3H), 2.57 (m, 1H), 3.10 (ABq, $J = 16$ Hz, $\delta\nu = 34.2$ Hz, 2H), 3.39 (m, 1H), 3.58 (m, 3H), 3.83 (m, 1H), 4.08 (d, $J = 17.6$ Hz, 1H), 4.39 (d, $J = 17.4$ Hz, 1H), 7.30 (m, 3H), 7.44 (d, $J = 5.9$ Hz, 1H), 7.76 (d, $J = 7.8$ Hz, 2H), 8.05 (d, $J = 8.4$ Hz, 1H); ¹³C NMR (CDCl₃, 100 MHz) δ 21.39, 24.20, 24.69, 24.87 (double intensity), 31.49, 31.54, 31.58, 32.43, 47.01, 52.19, 52.25, 52.49, 52.97, 55.63, 58.36, 127.65, 129.67, 135.28, 143.97, 167.52, 170.04, 172.84; MS (FAB, NBA-LiCl matrix): *m/z* (rel intensity) 526 (100) [M + Li]⁺, 370 (29) [M + Li − Ts]⁺. HRMS (NBA-LiCl) exact mass calcd for [C₂₅H₃₇N₅O₅S], 520.2594, found 520.2659.

(2*R*,3*R*,8*R*,9*R*)-Dicyclohexano-1,4,7,10,13-pentaazacyclopentadecane. (2*R*,3*R*,8*R*,9*R*)-Dicyclohexano-13-*p*-toluenesulfonyl-1,4,7,10,13-pentaazacyclopentadecan-5,11,15-trione (4.072 g, 7.84 mmol) was placed in a 1-L flask under an argon atmosphere, and dry 1,2-dimethoxyethane (dme, 220 mL) was added. The powder fused and did not appreciably dissolve. It was partially broken up with a spatula and stirred in a cold water bath, while lithium aluminum hydride (0.5

M in dme, 140 mL, 70 mmol) was added in portions over a 10 min period. Initially, the solution became cloudy, and undissolved chunks of compound were present. After about 70 mL had been added, the solution was fairly homogeneous, with only a few undissolved pieces remaining, which appeared to dissolve with gas evolution. Heating was started after a few minutes, and the solution rapidly became heterogeneous and yellow. The reaction mixture was refluxed overnight. Reflux was ended after 16.5 h. The reaction mixture was cooled in a cold water bath and then in a −18 °C bath. Water (2.2 mL) was added *cautiously* in small quantities over a 5−10 min period, followed more rapidly by 15% NaOH (2.2 mL) and then by water (6.6 mL). Stirring was continued for 2 h in the ice bath. Tetrahydrofuran (THF, 210 mL) was added, and stirring was continued for about an hour. The thick white suspension was allowed to settle and was filtered with a filter transfer device (#1 Whatman paper) under argon. The filtrate was stripped. The white residue was stirred with THF (150 mL) and filtered into the stripped first filtrate. The solvent was removed under reduced pressure, and the residue was placed on the vacuum line. The resulting yellow-white solid was extracted with hot dry hexane (initially 70 mL, 65 °C; then an additional 15 mL) and filtered through a filter transfer device (#50 Whatman paper) under argon, and the solvent was removed under reduced pressure. This crude product, weight about 1.5 g, was dissolved in hot (>70 °C) dry acetonitrile (about 60 mL), filtered (filter transfer device, #50 Whatman paper), concentrated by more than half, reheated to dissolve all of the white solid, and then allowed to cool slowly to room temperature all under argon. White crystals were obtained, 0.923 g, 2.85 mmol, 36.4% yield. ^{1}H NMR (C$_6$D$_6$, 300 MHz) δ 0.75−1.21 (several m, 8H), 1.23−2.19 (several m, 17H), 2.36−2.61 (several H, 6H), 2.61−2.73 (m, 2H), 2.74−2.85 (m, 2H), 2.90 (d, J = 7.5 Hz, 2H); ^{13}C NMR (C$_6$D$_6$, 75 MHz) δ 25.48, 25.56, 32.41, 32.48, 46.50, 47.82, 49.56, 61.86, 62.88. Anal. Calcd for C$_{18}$H$_{37}$N$_5$: C, 66.83; H, 11.54; N, 21.65. Found: C, 66.66; H, 11.46; N, 21.78.

N,N′-Bis(chloroacetyl)-(1S,2S)-diaminocyclohexane. (1S,2S)-Diaminocyclohexane (7.0 g, 61.13 mmol) was dissolved in 75 mL of alcohol free CHCl$_3$ in a four-neck, 2000 mL round bottom flask along with 38 mL of H$_2$O under argon. Two Normag dropping funnels were connected to the reaction flask and charged separately with chloroacetyl chloride (15 mL, 188.2 mmol) in alcohol free CHCl$_3$ (88 mL) and K$_2$CO$_3$ (24.2 g, 174.4 mmol) in H$_2$O (918 mL). An internal thermometer was inserted into the reaction flask. After cooling the two phase mixture in the reaction flask to 0 °C in an ice bath, the additions from the dropping funnels were started in such a way as to keep the proportion of each solution added approximately equal over a 1 h 30 min period. During the addition, an ice salt bath was used to moderate the temperature, keeping it between 3 and 0 °C. A shell of ice formed on the inside of the reaction flask which did not seem to impede the stirring. The reaction flask was removed from the ice bath at the end of the addition and was stirred for 2 h 15 min. The lower chloroform layer appeared to have a considerable quantity of a light solid in it at ice bath temperature, but it dissolved as the reaction warmed. The reaction mixture was placed in a separatory funnel, some additional chloroform was added, and the layers were separated. The aqueous layer was extracted with another portion of CHCl$_3$ (150 mL), and the combined chloroform layers were washed with water (100 mL), then saturated aqueous NaCl (150 mL), dried (Na$_2$SO$_4$), and stripped down to an off-white solid. This solid was stirred for 2 days with about 500 mL of ether and then filtered, much of the color staying in the ether, giving a white solid, 14.14 g, 53.33 mmol, 87.0% yield, mp 230−231 °C. ^{1}H NMR (CDCl$_3$, 400 MHz) δ 1.34 (m, 4H), 1.80 (m, 2H), 2.08 (m, 2H), 3.75 (m, 2H), 3.99 (ABq, J = 15.0 Hz, δν = 8.1 Hz, 4H), 6.78 (br s, 2H); ^{13}C NMR (CDCl$_3$, 100 MHz) δ 24.53, 31.99, 42.41, 53.85, 166.66; HRMS (FAB+, GT-HCl) exact mass calcd for [C$_{10}$H$_{16}$Cl$_2$N$_2$O$_2$ + H$^+$], 267.0667; found 267.0652.

(2S,3S,8R,9R)-Dicyclohexano-13-*p*-toluenesulfonyl-1,4,7,10,13-pentaazacyclopentadecan-5,11,15-trione. N-*p*-Toluenesulfonylglycyl-(1R,2R)-diaminocyclohexane (3.4 g, 10.44 mmol) and the N,N′-bis(chloroacetyl)-(1S,2S)-diaminocyclohexane (2.79 g, 10.44 mmol) were combined in a 3-L flask, and dry N,N′-dimethylacetamide (1.95 L) was added. After inerting the flask, sodium hydride (95%, 0.559 g, 22.1 mmol) and an additional portion of N,N′-dimethylacetamide (100 mL) were added. The reaction flask was placed in an oil bath at 71 °C. After the internal temperature reached 60 °C, gas evolution

became constant. About 1 h later, the internal temperature was 64 °C. After stirring overnight, the reaction mixture became homogeneous. Heating was stopped after 20 h and allowed to cool. Some white solid product was present, which was filtered off. After drying, this portion weighed 1.34 g. The filtrate was concentrated under reduced pressure until a yellow solid was obtained. This solid was treated with dichloromethane (600 mL) and washed with water (100 mL, twice) and then with saturated aqueous sodium chloride (twice, 100 mL). The combined aqueous layers were backwashed with dichloromethane (150 mL). The combined organic layers were dried (sodium sulfate), filtered, and stripped down to a pale yellow solid. This solid was stirred in methanol at 50−55 °C for 1.5 h and then allowed to reach room temperature overnight. After filtration 1.0 g of a white product was recovered by filtration, and a subsequent 0.071 g was recovered from the filtrate, giving a total of 2.41 g (44.4% yield), mp 305−306 °C. ^{1}H NMR (CDCl$_3$ + CD$_3$OD (four drops), 400 MHz) δ 1.0−1.5 (several m, 7H), 1.67−2.07 (several m, 9H), 2.81 (td, J = 10.2, 3.2 Hz, 1H), 2.91−3.06 (d and m, J = 17.2 Hz, 2H), 3.4−3.74 (several m, 5H), 3.92 (d, J = 17.7 Hz, 1H), 4.05 (d, J = 17.0 Hz), 7.35 (d, J = 8.1 Hz, 2H), 7.75 (d, J = 8.3 Hz, 2H); ^{13}C NMR (CDCl$_3$ + CD$_3$OD (four drops), 100 MHz) δ 21.56, 24.59, 24.93, 25.01, 25.19, 30.35, 31.31, 32.21, 33.21, 51.49, 52.81, 53.32, 53.99, 54.49, 57.95, 58.51, 127.69, 129.97, 134.76, 144.49, 168.54, 169.35, 173.01; HRMS (FAB+, GT-HCl) exact mass calcd for [C$_{25}$H$_{37}$N$_5$O$_5$S + H$^+$], 520.2594; found 520.2605.

(2S,3S,8R,9R-Dicyclohexano-1,4,7,10,13-pentaazacyclopentadecane. The (2S,3S,8R,9R)-dicyclohexano-13-*p*-toluenesulfonyl-1,4,7,10,13-pentaazacyclopentadecan-5,11,15-trione (2.176 g, 4.187 mmol) was suspended in dry 1,2-dimethoxyethane (dme, 175 mL) in a 1000 mL round bottom flask and inerted with argon. While this solution was stirred in an ice water bath, lithium aluminum hydride in dme (0.5 M, 86 mL, 43 mmol) was rapidly added with a syringe over a 2−3 min period. There was considerable gas evolutio,n and the solution became heterogeneous. After stirring for about 15 min, the ice water bath was removed and replaced with a heating mantle. Over the next 15 min the reaction mixture was heated to reflux becoming bright (opaque) yellow. After refluxing for several hours the yellow color faded somewhat. After refluxing for 24 h, the faded yellow mixture was allowed to cool. It was placed in an ice bath, and water (1.4 mL) was *cautiously* added dropwise over about 2 min with considerable gas evolution. Aqueous 15% NaOH (1.4 mL) was added, followed by more water (4.0 mL). This thick mixture was stirred for about 30 min, and then tetrahydrofuran (100 mL, passed through a column of basic alumina) was added. The mixture was stirred for about 2 h and then filtered using a filter transfer device under argon. The filtrate was removed under reduced pressure and placed on the vacuum line, giving 1.13 g of a white solid. This was dissolved in hot dry hexanes (100 mL) and filtered using a filter transfer device. The small amount of solid left behind was washed with 40 mL more hexanes. The hexane was removed under reduced pressure, leaving a cream colored solid which was recrystallized from hot acetonitrile under argon, 0.622 g, 1.92 mmol, 46% yield. ^{1}H NMR (CDCl$_3$, 400 MHz) δ 0.96 (m, 4H), 1.22 (m, 4H), 1.63−2.18 (several m, 17H), 2.47−2.69 (several m, 6H), 2.75 (m, 2H), 2.87 (m, 2H), 2.95 (m, 2H); ^{13}C NMR (CDCl$_3$, 100 MHz) δ 25.13, 25.20, 31.99, 32.15, 45.78, 45.94, 48.66, 61.17, 61.65; HRMS (FAB$^+$, glycerol; TFA; PEG-300) exact mass calcd for [C$_{18}$H$_{37}$N$_5$ + H$^+$], 324.3127; found, 324.3142.

Syntheses of Complexes: Manganese(II) Dichloride (2R,3R,8R,9R-Dicyclohexano-1,4,7,10,13-pentaazacyclopentadecane (3). A methanol solution (35 mL) of the free base (2R,3R,8R,9R)-dicyclohexano-1,4,7,10,13-pentaazacyclopentadecane, (5.80 g, 17.93 mmol) was added to a hot methanolic solution (100 mL) containing 2.25 g (17.9 mmol) of anhydrous manganese(II) chloride. The solution was refluxed under a dry nitrogen atmosphere for 1 h and then stirred for an additional 12 h at room temperature. After cooling, the solution was taken to dryness, and the solid mass was dissolved in 50 mL of hot (~60 °C) THF. The solution was filtered through Celite and concentrated *in vacuo* to dryness. Ethyl ether was added to the solid mass which was then vigorously stirred. White crystals were collected by filtration, washed with ether, and dried to give 7.30 g (91% yield) of **3**: [α]$^{20}_D$ = −96.97° (c = 0.02, methanol); MS (FAB, NBA matrix) m/z (rel intensity): 448.1 (M$^+$, 2), 413.2 [(M − Cl, 100)$^+$]. Anal. Calcd for C$_{18}$H$_{37}$Cl$_2$-

MnN$_5$: C, 48.11; H, 8.30; N, 15.59; Cl, 15.78. Found: C, 48.23; H, 8.32; N, 15.47; Cl, 15.73.

Manganese(II) Dichloride (2*R***,3***R***,8***S***,9***S***-Dicyclohexano-1,4,7,10, 13-pentaazacyclopentadecane (4).** To a hot methanol solution containing 186 mg (1.474 mmol) of anhydrous manganese(II) chloride was added the free base (477 mg, 1.474 mmol) under a dry N$_2$ atmosphere. The reaction was carried out identically to that described for complex **3**. After drying *in vacuo* a yield of 0.56 g (84%) was obtained; MS (FAB, NBA matrix) *m/z* (rel intensity): 448.1 (M$^+$, 1), 413.2 [(M − Cl, 100)$^+$. Anal. Calcd for C$_{18}$H$_{37}$Cl$_2$MnN$_5$: C, 48.11; H, 8.30; N, 15.59; Cl, 15.78. Found: C, 48.34; H, 8.17; N, 15.65; Cl, 15.70.

Manganese(II) 1,4,7,10,13-Pentaazacyclopentadecane Bis(nitrate) (6). To 50 mL of warm methanol solution containing 0.605 g (0.233 mmol) of Mn(NO$_3$)$_2$·*x*H$_2$O (21% Mn) was added 0.50 g of the ligand 1,4,7,10,13-pentaazacyclopentadecane. The solution was refluxed for 1 h and reduced in volume to ∼10 mL. At this point diethyl ether was added to the cloud point (∼20 mL). The solution was allowed to sit undisturbed for 2 days whereupon very large clear white crystals had formed. The solid was collected by filtration, washed with diethyl ether, and dried overnight in vacuo. The yield of the complex **6** was 0.80 g (73% of theory). MS (FAB, NBA matrix) *m/z* (rel intensity): 332 [(M(L)(NO$_3$), 100)$^+$. Anal. Calcd for C$_{10}$H$_{25}$MnN$_7$O$_6$: C, 30.46; H, 6.39; N, 24.87. Found: C, 30.70; H, 6.33; N, 24.66.

Physical Methods. Stability constants for the two new dicyclohexano) complexes, **3** and **4**, were obtained by utilizing standard potentiometric titration methods as first described by Martell et al.,[5] and further described in detail in our previous studies.[2] Kinetic stabilities were determined by the Cu(II) ion competition method described in detail in our previous studies.[2] The method utilized to determine the superoxide dismutase catalytic activity of the Mn(II) complexes reported here is based on the stopped flow kinetic assay described previously.[1,2,3a,6] The work described here utilized the same methodology, and the k_{cat} for each complex was assessed over the pH range of 7.4−8.3.

X-ray Crystal Structures. Single crystals of **4·**C$_2$H$_5$OH were collected on a computer-controlled Nicolet autodiffractometer using Θ−2Θ scans and nickel-filtered CuK$_\alpha$ radiation with a total of 4050 independent absorption-corrected reflections having 2Θ (CuK$_\alpha$) < 120° (the equivalent of 0.65 limiting CuK$_\alpha$ spheres). The structure was solved using "Direct Methods" techniques with the Siemens SHELXTL-PC software package as modified at Crystalytics Company. The resulting structural parameters were refined to convergence {R_1 (unweighted, based on F) = 0.058 for 1611 independent absorption-corrected reflections having 2 Θ (CuK$_\alpha$) < 120° and $I > 3s(I)$} using counter-weighted full-matrix least-squares techniques and a structural model which incorporated anisotropic thermal parameters for all but three (O$_{1s'}$, C$_{1s'}$, and C$_{2s'}$) non-hydrogen atoms and isotropic thermal parameters for these three non-hydrogens and all included hydrogen atoms. The hydrogen atoms included in the structural model were fixed at idealized sp^3-hybridized positions with C−H and N−H bond lengths of 0.96 and 0.90 Å, respectively. The ethanol solvent molecule of crystallization is disordered in the lattice with (at least) two alternate positions for each of its nonhydrogen atoms. The oxygen atoms are distinguished from the carbons based on the favorable hydrogen-bonding interactions in the lattice; the following factors were employed in all structure factor calculations: O$_{1s}$, 0.80; O$_{1s'}$, 0.20; C$_{1s}$, 0.65; C$_{1s'}$, 0.35; C$_{2s}$, 0.60; C$_{2s'}$, 0.40. Since none of these solvent non-hydrogen atoms could be satisfactorily refined as independent atoms, they were constrained to have common C−O and C−C bond lengths which refined to final values of 1.336 and 1.439 Å, respectively. The intramolecular C···O separations between terminal non-hydrogen solvent molecule atoms were also constrained to be 1.633 times the value of the common C−O bond length.

Single crystals of **6** were collected on a Siemens R3m/V diffractometer at −100 °C using 2Θ−Θ scans and MoK$_\alpha$ radiation with a total of 2464 independent semiempirical absorption corrected reflections collected with a 2Θ range from 3.5 to 55.0 °C. The structure was solved using "Heavy Atom Methods" with the Siemens SHELXTL PLUS (VMS) software package. The resulting structural parameters were refined to convergence {R_1(unweighted) = 2.09% for 2192 independent absorption-corrected reflections} using full matrix least-
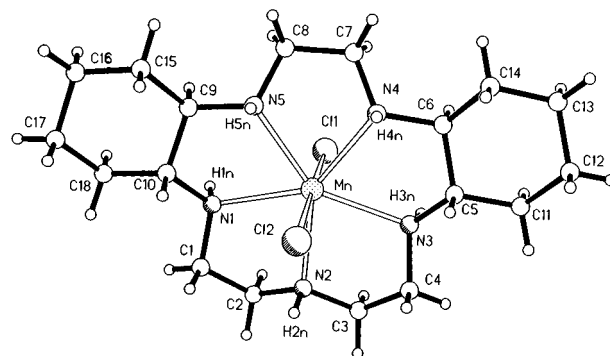

Figure 2. ORTEP drawing for manganese(II) dichloride (2*R*,3*R*,8*S*,9*S*)-dicyclohexano-1,4,7,10,13-pentaazacyclopentadecane (**4**) showing the labeling scheme and the 50% probability ellipsoids for non-hydrogen atoms.

squares techniques with hydrogen atoms positionally refined with common isotropic *U*.

Results and Discussion

Previously we reported that complex **2**, containing a single *trans*-fused cyclohexano ring, is both a more active SOD catalyst than **1**, and it possesses an enhanced chemical stability toward dissociation of the Mn(II) ion as compared to **1**. The point of this prior work was to identify those substituents and substituent patterns which would allow us to maximize the stability of the corresponding Mn(II) complex and at the same time retain the catalytic activity. From this exercise the *trans*-cyclohexano moiety emerged as the best substituent for accomplishing this dual function. In this paper we describe our efforts to probe the additivity of the beneficial effects arising from the *trans*-fused cyclohexano moiety by synthesizing ligands containing multiple *trans*-fused cyclohexano substituents. We report here two new isomeric bis(*trans*-fused cyclohexano) ligands (2*R*,3*R*,8*R*,9*R* and 2*R*,3*R*,8*S*,9*S* stereochemistries) and their Mn(II) complexes, **3** (2*R*,3*R*,8*R*,9*R*) and **4** (2*R*,3*R*,8*S*,9*S*). The new complexes, **3** and **4**, were synthesized by reacting the ligands with anhydrous MnCl$_2$ in MeOH under dry N$_2$. Additionally, the new bis(nitrate) complex **6**, derived from the ligand of complex **1**, was synthesized by reacting the ligand with anhydrous Mn(NO$_3$)$_2$ in dry methanol under N$_2$. The molar conductances of each of the white complexes, **3**, **4**, and **6**, were measured in methanol, and all were consistent with a 1:1 electrolyte type implying either a six-coordinate [Mn(L)X]$^+$ or solvated seven-coordinate structure, [Mn(L)(MeOH)X]$^+$ in solution. Magnetic susceptibilities measured by the Evan's method in methanol solution were consistent with these complexes existing as high-spin d^5 complexes.[7] The cyclic voltammetry of each of these new complexes, **3** and **4**, exhibits a well-defined reversible one-electron oxidation at E$_{1/2}$ at 0.74 V vs SHE in anhydrous methanol containing 0.25 M *n*-Bu$_4$-NBF$_4$.

X-ray Diffraction and Crystal Structures. Complex **4** was shown by single-crystal X-ray diffraction to have a seven-coordinate structure (Figure 2) analogous to other Mn(II) complexes of this class.[1,2,8] In Tables 1 and 2 are reported some pertinent bond length and bond angle data, respectively. Additional data are reported in the Supporting Information. The structure is fairly typical for this class of pentaaza macrocyclic complexes of Mn(II). The ClMnCl bond angle is 177.2°, and

(5) Martell, A. E.; Motekaitis, R. J. *Determination and Use of Stability Constants*, 2nd ed.; VCH Publishers, Inc.: New York, 1992; p 29.
(6) Riley, D. P.; Rivers, W. J.; Weiss, R. H. *Anal. Biochem.* **1991**, *196*, 344.
(7) Evans, D. F. *J. Chem. Soc.* **1959**, 2003.
(8) Neumann, W. L.; Franklin, G. W.; Sample, K. R.; Aston, K. W.; Weiss, R. H.; Riley, D. P. *Tetrahron Lett.* **1997**, *38*, 779.

Table 1. Crystal Data for Complex **4**

specimen	colorless, rectangular paralellopiped, 0.15 × 0.22 × 0.85 mm
crystal system	triclinic, at 20 °C
space group	P_1-C_i2 (no. 2)
formula	$C_{18}H_{37}Cl_2MnN_5 \cdot C_2H_5OH$
a, Å	9.746(3)
b, Å	12.631(6)
c, Å	11.311(5)
α, deg	73.14(4)
β, deg	76.39(3)
γ, deg	79.98(3)
V, Å	1287(1)
ρ_{calc}, g/cm^3	1.279
Z	2
f_w	495.43
λ, Å	1.54184
diffractometer	Four-Circle Nicolet (Siemens) Autodiffractometer
radiation (Å)	nickel-filtered CuK_α
data collection	$\Theta - 2\Theta$
reflections$_{tot}$	4050
obsd data, $I > 3\sigma(I)$	1611
abs. coeff, mm^{-1}	6.23
goodness of fit	1.59
$R = \Sigma||F_0| - |F_c||/\Sigma|F_0|$	0.058
$R_w = \{\Sigma w(|F_0| - |F_c|)^2/ \Sigma w|F_0|^2\}^{1/2}$	0.069

Table 2. Crystal Data for Complex **6**

specimen	colorless prism, 0.22 × 0.42 × 0.64 mm
crystal system	orthorhombic, at 20 °C
space group	$P2_12_12_1$
formula	$C_{10}H_{25}MnN_6O_3 \cdot NO_3$
a, Å	9.457(2)
b, Å	12.758(2)
c, Å	13.834(2)
V, Å^3	1669.1(5)
ρ_{calc}, g/cm^3	1.549
Z	4
f_w	389.3
λ, Å	0.710 73 Å
diffractometer	Siemens R3m/V
data collection	$\Theta - 2\Theta$
reflections$_{tot}$	2652
obsd data, $I > 3\sigma(I)$	2192
abs. coeff	semiempirical
goodness of fit	1.20
$R = \Sigma||F_0| - |F_c||/\Sigma|F_0|$	0.0283
$R_w = \{\Sigma w(|F_0| - |F_c|)^2/\Sigma w|F_0|^2\}^{1/2}$	0.0381

Table 3. Selected Bond Lengths (Å) for Complexes **4** and **6**

complex **4**		complex **6**	
type	length	type	length
Mn−Cl$_1$	2.560(4)	Mn−O$_1$	2.222(2)
Mn−Cl$_2$	2.631(4)	Mn−N$_1$	2.277(2)
Mn−N$_1$	2.366(7)	Mn−N$_2$	2.281(3)
Mn−N$_2$	2.308(9)	Mn−N$_3$	2.273(2)
Mn−N$_3$	2.313(7)	Mn−N$_4$	2.308(2)
Mn−N$_4$	2.319(8)	Mn−N$_5$	2.275(3)
Mn−N$_5$	2.338(8)		

this very nearly linear angle is similar to that observed in the structure for **1** indicating that the steric bulk of the *trans*-fused cyclohexano substituents is minimally sensed by the axial ligands. In contrast the ClMnCl angle in the 2,2,3,3-tetramethyl complex[2] is 167° indicating that the axial methyl groups do indeed exert an axial steric effect. The five nitrogen atoms and the Mn(II) ion are also very nearly coplanar. Additionally, the Mn−N and Mn−Cl bond lengths are similar to those values observed in **1** and other complexes in this class.

The crystal structure of complex **6** is illustrated in Figure 3 and is in marked contrast to other structures in this series. Replacing the chloride counterions with nitrate has made it possible to crystallize a six-coordinate complex with the unsubstituted pentaaza ligand of structure **1**. The resultant complex **6** has a Mn(II) ion in a six-coordinate distorted
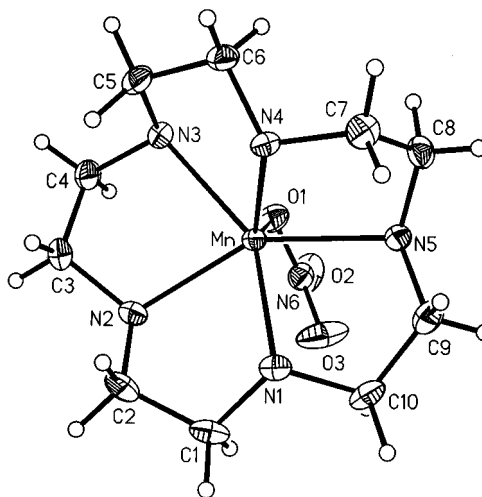
Figure 3. ORTEP drawing for manganese(II) (1,4,7,10,13-pentaaza-cyclopentadecane Bis(nitrate) (**6**) showing the labeling scheme and the 50% probability ellipsoids for the non-hydrogen atoms.

Table 4. Selected Bond Angles (deg) for complexes **4** and **6**

complex **4**		complex **6**	
type	angle	type	angle
Cl$_1$MnCl$_2$	177.2(1)	O$_1$MnN$_1$	128.6(1)
Cl$_1$MnN$_1$	85.4(2)	O$_1$MnN$_2$	93.3(1)
Cl$_1$MnN$_2$	96.4(2)	O$_1$MnN$_3$	78.0(1)
Cl$_1$MnN$_3$	85.2(2)	O$_1$MnN$_4$	132.0(1)
Cl$_1$MnN$_4$	93.5(2)	O$_1$MnN$_5$	92.5(1)
Cl$_1$MnN$_5$	97.4(2)	N$_1$MnN$_2$	76.5(1)
Cl$_2$MnN$_1$	93.9(2)	N$_2$MnN$_3$	77.7(1)
Cl$_2$MnN$_1$	80.9(2)	N$_3$MnN$_4$	76.1(1)
Cl$_2$MnN$_3$	93.9(2)	N$_4$MnN$_5$	76.7(1)
Cl$_2$MnN$_4$	88.7(2)	N$_5$MnN$_1$	76.9(1)
Cl$_2$MnN$_5$	84.9(2)		

octahedral coordination geometry with the N^4 occupying a site which approximates a *trans* position in an octahedral geometry. The resultant N^{4}MnO bond angle is 132.0°. This structure is seemingly intermediate between the planar macrocyclic ligand conformation and a folded array with the idealized N^{4}MnO angle of 180°. Thus, while the structure is distorted from true octahedral, it nevertheless shows that the ligand has adopted a folded geometry in which one of the nitrogens is considerably displaced from the plane of the Mn(II) ion and the remaining four nitrogens. The Mn−N bond lengths are somewhat shorter than those observed in both complex **1** and **4**; e.g., the average Mn−N bond length in **6** (2.28 Å) is less than that observed with either **4** (2.33 Å) or **1** (2.36 Å).

Stability Studies. The stabilities of the two new bis(*trans*-fused) cyclohexano complexes, **3** and **4**, were assessed for both their thermodynamic and kinetic stabilities via the potentiometric titration method and the Cu(II) ion competition method, respectively (see Experimental Section). The log *K* value for **3** was slightly greater than that measured for **4**: 13.6 versus 13.5 and the corresponding kinetic stability of **3** was also slightly greater than that observed with **4**. The second-order rate constant, k_{diss}, at 21 °C for the proton-assisted dissociation of each complex (first-order in [complex] and first-order in [H$^+$]), was measured to be 28 M^{-1} s^{-1} for **3** and 31.5 M^{-1} s^{-1} for **4**. If one considers the kinetic stability at a given pH, then the first-order rate of loss of ligand from the metal is calculated by multiplying k_{diss} by the [H$^+$]; e.g., for **3** at pH = 7 the rate is 2.8×10^{-7} s^{-1} which gives a half-life to equilibrium at this pH of about 690 h.[9] For comparison the kinetic stability enhance-

(9) The kinetics of dissociation of the ligand at any fixed pH is first-order in complex; thus, at a given pH the second-order rate constant can be converted to a half-life value by the following equation: $t_{1/2} = 0.694/(k_{diss} \times [H^+])$.

ment for **3** over complex **1** is approximately ~1125-fold. From the potentiometric titration data, the complex **3** is completely intact down to a pH as low as 6.1; thus, at pH = 7.4 there is no free Mn(II) in the stoichiometric presence of this ligand and hence this complex is quite stable under normal physiological conditions. It is also important to compare the log K for **3** to the parent unsubstituted complex **1** and the mono *trans*-fused cyclohexano complex **2**. Clearly, the two cyclohexano rings are acting synergistically to enhance the stability of the complex, since **3** is nearly 600 times more stable than **1** and nearly 60 times more stable than **2**.
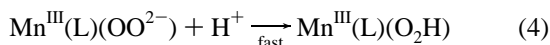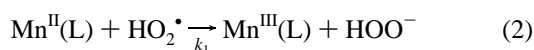
Kinetic Studies. Each complex was evaluated as an SOD catalyst over a range of pH's.[6] While complex **6** was identical to that of the dichloro analogue **1**, the k_{cat} observed for the two bis (*trans*-fused) cyclohexano derivatives, **3** and **4**, provided us with some very intriguing results; namely, **3** is over three times faster than **1** at pH = 7.4: $k_{cat} = 1.21 \times 10^{+8}$ M^{-1} s^{-1}, functioning at a rate equivalent to native mitochondrial Mn-SOD enzyme,[6] while complex **4** exhibits no detectable SOD activity. This very striking contrast in the catalytic rate of superoxide dismutation for these two steroisomeric complexes dramatically demonstrates the need to understand how substituents affect the rate.

For complex **3** the catalytic rate of dismutation of superoxide, k_{cat}, is first-order in [O$_2^{\bullet-}$] and [**3**]$_{added}$. The [H$^+$] dependence for SOD catalysis exhibits a linear dependence on the [H$^+$] from pH = 7.4−8.6 (Supporting Information).[1] A [H$^+$] independent pathway is observed ($k_{ind} = 3.16 \times 10^7$ s^{-1}, $k_2 = 1.58 \times 10^7$ s^{-1}) such that the observed rate law is shown in eq 1

$$V = -d[O_2^{\bullet-}]/dt = [Mn]^1_{tot}[O_2^{\bullet-}]^1\{k_{H+}[H^+]^1 + k_{ind}\} \quad (1)$$

where $k_{H+} = 2k_1/K_a$, $k_{ind} = 2k_2$ and K_a is the acidity constant for superoxide ($K_a = 2.04 \times 10^{-5}$).[10]

At 21 °C, k_{H+} was found from the slope of the k_{cat} vs [H$^+$] plot to be 2.24×10^{15} M^{-1} s^{-1}, which affords a calculated value of $k_1 = 2.25 \times 10^{10}$ M^{-1} s^{-1}. These results indicate that **3** operates via a mechanism similar to the other complexes in this series with oxidation of Mn^{II}(L) being rate-limiting in the catalytic process (eqs 2−4),[1] although **3** does so with faster rates: e.g., for **1**: $k_2 = 0.91 \times 10^{-7}$ s^{-1} and $k_1 = 0.29 \times 10^{10}$ M^{-1} s^{-1}, for **2**: $k_2 = 1.44 \times 10^7$ s^{-1} and $k_1 = 0.78 \times 10^{10}$ M^{-1} s^{-1}.[2]

$$Mn^{II}(L) + HO_2^{\bullet} \xrightarrow{k_1} Mn^{III}(L) + HOO^- \quad (2)$$

$$Mn^{II}(L) + O_2^{\bullet-} \xrightarrow{k_2} Mn^{III}(L)(OO^{2-}) \quad \text{(inner-sphere)} \quad (3)$$

$$Mn^{III}(L)(OO^{2-}) + H^+ \xrightarrow{fast} Mn^{III}(L)(O_2H) \quad (4)$$

To aid design efforts, we set out to gain added insight into the details of the rate-limiting electron-transfer steps by studying the kinetics of the dismutation of O$_2^{\bullet-}$ in D$_2$O with **3** and the 2S,5R,8S,11R,14S-pentamethyl complex, **5**,[2] which exhibits no [H$^+$] dependence in its SOD activity ($k_2 = 1.91 \times 10^7$ s^{-1}). The catalytic rate for O$_2^{\bullet-}$ dismutation with both **3** and **5** in D$_2$O over the pH range of 7.4−8.6[11] exhibits similar kinetic behavior to that oberved in H$_2$O; namely, **5** exhibits a pH independent rate which was decreased ~45%: $k_2 = 1.01 \times 10^7$ s^{-1}. In contrast, **3** also displays a rate change in D$_2$O, with k_1 decreased by ~50%, but k_2 increased by ~10%: $k_1 = 1.07 \times 10^{10}$ M^{-1} s^{-1} and $k_2 = 1.83 \times 10^7$ s^{-1}.

These results, combined with the observations that **4** is not a catalyst, that **5** has no pH dependent component to its k_{cat}, and that the proton-dependent electron-transfer rate constants for **1**, **2**, and **3** are approaching diffusion controlled limits, lead to

some important insights. First, the rate of the pH independent path is consistent with an S$_N$1 (bond-breaking) process in which creation of the vacant axial coordination site on Mn(II) is rate-limiting, followed by rapid binding of superoxide anion to Mn(II) (eq 2) and then rapid protonation/oxidation of the resultant Mn(II)-superoxo complex yielding the Mn(III)hydroperoxo complex. This pH independent pathway exhibits a modest deuterium isotope effect for both **3** and **5**, suggesting that creation of the vacant coordination site by loss of coordinated water is involved in the rate-determining step. The sign and magnitude are not readily rationalized, as solvent exchange rates on metal ions can be both faster and slower in D$_2$O than in H$_2$O,[12] but that there is an effect indicates the involvement of aquo ligand exchange in the rate-determining step. The rate of loss of water from the inner-coordination sphere of aquo Mn(II) has been measured to be 0.8×10^7 s^{-1},[13] and such a value similar to that observed here for k_2 provides additional support for this mechanistic interpretation. Finally, a weakly binding counterion such as chloride should act as a competitive inhibitor and hence decrease the rate in a linear fashion with added chloride. When the k_{cat} for complex **5** was measured at pH = 7.8 with [Cl$^-$]$_{added}$ over the range from 0−250 μM, the k_{cat} decreased linearly from 3.82×10^7 to 2.61×10^7 M^{-1} s^{-1} consistent with competitive binding with superoxide to Mn(II) in this pH independent pathway.

A second conclusion is that the near diffusion-controlled rate of the pH dependent electron-transfer process requires that the barrier to electron transfer to HO$_2^{\bullet}$ be minimal.[14] This implies that no charge separation develops in the transition state and that the reorganizational energy be minimal;[15] i.e., the Mn(III) and Mn(II) complexes are similar in structure. This means that the precursor Mn(II) complex must possess a six-coordinate pseudo-octahedral geometry resembling the six-coordinate octahedral geometry of Mn(III), regardless of the oxidation pathway involved.

The results observed for the pH dependence on the rate in D$_2$O are consistent with these conclusions. The rate drop observed for **3** in D$_2$O is similar to that observed for the Fe^{II}/Fe^{III} self-exchange in water in which an isotope effect of 2 is observed for the process involving a H-atom transfer from a bound water on Fe(II).[16−18] While the small magnitude of the effect does not provide an overwhelmingly compelling case for H-atom transfer,[19] it is important to note that this apparent kinetic isotope effect in our system has an equilibrium isotope effect component. At any pH weak acids generally are dissociated to a greater extent in light water than in D$_2$O (e.g., $K_{HOAc}/K_{DOAc} \sim 3.3$),[20] thus, the actual [DO$_2^{\bullet}$] will be greater than [HO$_2^{\bullet}$] by a factor of approximately 3. Factoring in this increased concentration of DO$_2^{\bullet}$ relative to HO$_2^{\bullet}$ means that

(10) Sawyer, D. T.; Valentine, J. S. *Acc. Chem. Res.* **1981**, *14*, 393.
(11) Covington, A. K.; Paabo, M.; Robinson, R. A.; Bates, R. G. *Anal. Chem.* **1968**, *40*(3), 501.
(12) (a) Reidler, J.; Silber, H. B. *J. Phys. Chem.* **1973**, *77*, 1275. (b) Sutin, N.; Rowley, J. K.; Dodson, *J. Phys. Chem.* **1961**, *65*, 1248. (c) Bunn, D.; Dainton, F. S.; Duckworth, S. *Trans. Faraday Soc.* **1961**, *57*, 1131.
(13) Eigen, M. *Pure Appl. Chem.* **1963**, *6*, 105.
(14) Marcus, R. A. *Annu. Rev. Phys. Chem.* **1964**, *15*, 155.
(15) a) Macartney, D. H.; Thompson, D. W. *Inorg. Chem.* **1989**, *28*, 2199. (b) Endicott, J. F.; Kumar, K.; Ramasami, T.; Rotszinger, F. P. In *Progress in Inorganic Chemistry*; Lippard, S. J., Ed., Wiley: New York, 1993; Vol. 30, p 141. (c) Creaser, I. I.; Harrowfield, J. M.; Herlt, J.; Sargeson, A. M.; Springborg, J.; Geue, R. J.; Snow, M. R. *J. Am. Chem. Soc.* **1977**, *99*, 3181.
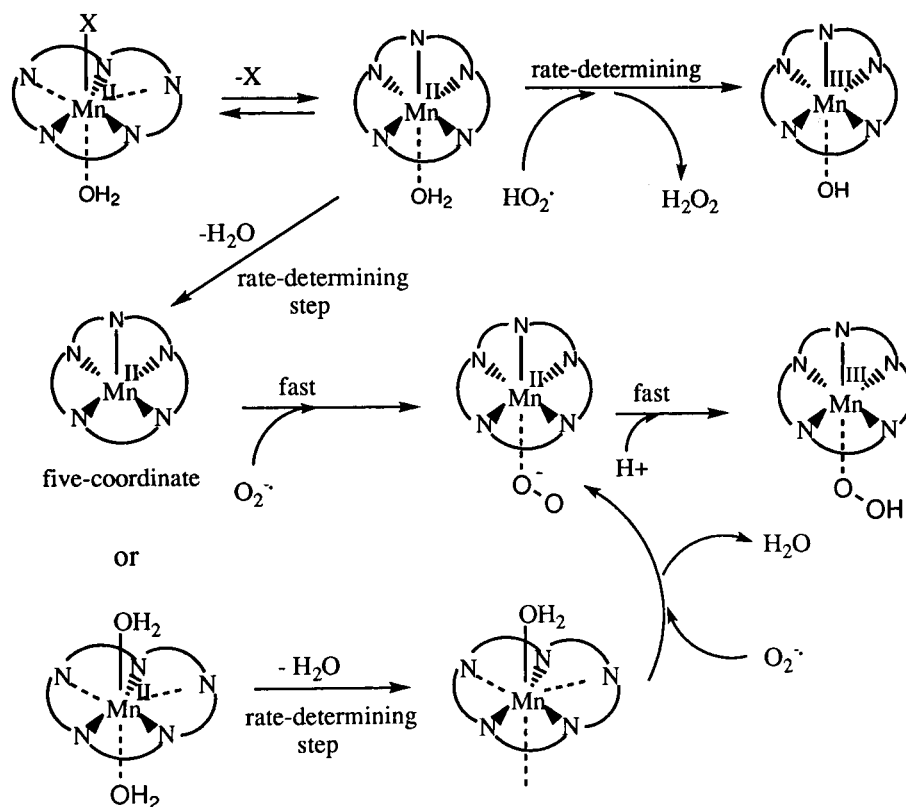(16) Hudis, J.; Dodson, R. W. *J. Am. Chem. Soc.* **1956**, *78*, 911.
(17) Friedman, H.; Newton, M. *J. Electroanal. Chem.* **1986**, *204*, 21.
(18) Reynolds, W. L.; Lumry, R. W. *J. Chem. Phys.* **1955**, *23*, 2460.
(19) Kresge, A. J. *Sixth Steenbock Symposium on Isotope Effects on Enzyme Catalyzed Reactions*; Cleland, W. W., O'Leary, M. H., Northrop, D. B., Eds.; University Park Press: Baltimore, 1977; pp 37−63. (b) Westheimer, F. H. *Chem. Rev.* **1961**, *61*, 265.

Scheme 1

the actual kinetic isotope effect is ~ 6—a value more in keeping for H-atom transfer.[19]

Folding of the macrocyclic ring so that one of its secondary amines occupies an axial site generating a pseudo-octahedral complex, $[Mn^{II}(L)X]^{n+}$, is a structural motif which accommodates this mechanistic picture. It is for this reason that the crystal structure of complex **6** is significant. This six-coordinate complex exhibiting the partially folded ring motif confirms that stable pseudo-octahedral geometries are to be expected within this class of complex and can conceivably play a major role in the redox activity of the Mn center. Thus, if the macrocyclic [15]aneN$_5$ ligand possesses C-substituents which, due to intramolecular steric repulsions and angle strains, could force the ligand to adopt a folded pseudo-octahedral geometry about the spherically symmetrical Mn(II) ion, then the Mn(II) complex would be poised to undergo facile electron-transfer. In the scheme the two pathways for the rate-determining oxidation of Mn(II) to Mn(III) are depicted. The important features are that the outer-sphere path proceeds through an intermediate pseudo-octahedral $[Mn^{II}(L)(H_2O)]^{2+}$ complex with a folded macrocyclic ligand, while the inner-sphere substitution pathway would involve a superoxo $[Mn^{II}(L)(O_2{}^\bullet)]^+$ six-coordinate intermediate complex, containing the folded macrocyclic ligand, which would be protonated to generate the $[Mn^{III}(L)(HO_2)]^{2+}$ pseudo-octahedral complex.

Thus, by affecting the degree of *folding* of the macrocyclic ligand, the position, number, and stereochemistry of the substituents could reasonably be expected to exert a major effect on the rate of electron-transfer via the pH dependent H-atom transfer pathway. This need to fold the ligand into a conformation which will stabilize a pseudo-octahedral geometry on Mn(II)

may be the reason why complex **5**, for example, shows no rate for this pH dependent pathway. It is intriguing to speculate that the steric constraints imposed on this complex by the presence of a methyl substituent symmetrically positioned on one carbon of each chelate ring may inhibit folding and thereby block this pathway for electron-transfer. This implies that the two pathways may operate by different folding motifs. We are continuing to explore this substituent effect via a combination of molecular mechanics calculations and synthesis with the goal of rational design of highly substituted chemically stable synthetic enzymes.

Note Added in Proof: Recent studies provide additional support for a proton-coupled electron transfer (as discussed herein) as an important pathway of electron transfer in biological systems such as photosystem II,[21] as this path does not require charge separation to build up in the transition state. Additionally, a recent report indicates that the thermodynamics of an H-atom transfer from a Mn-bound water to HO$_2{}^\bullet$ will be favorable; i.e., the bond dissociation energy (BDE) of an O–H bond of a water bound to a Mn(III)(Salen) derivative is 86 kcal/mol.[22] Thus, H-atom transfer to HO$_2{}^\bullet$ is energetically allowed as the BDE of the O–H bond of hydrogen peroxide is reported to be 87.2 kcal/mol.[23]

Supporting Information Available: Figure showing the measured k_{cat} as a function of pH for the complex **3** and crystallographic details for complexes **4** and **6** (including atomic coordinates, anisotrophic thermal parameters, bond lengths, and bond angles for non-hydrogen atoms) (15 pages). See any current masthead page for ordering and Internet access instructions.

(20) Swain, C. G.; Bader, R. F. W.; Thorton, E. R. *Tetrahedron* **1960**, *10*, 200.

(21) Haganson, C. W.; Lydakis-Simantris, N.; Tang, X.; Tommos, C.; Warncke, K.; Babcock, G. T.; Diner, B. A.; McCracken, J.; Styring, S. *Photosynth. Res.* **1995**, *46*, 177.

(22) Caudle, M. T.; Pecoraro, V. L. *J. Am. Chem. Soc.* **1997**, *119*, 3415.

(23) Howard, C. J. *J. Am. Chem. Soc.* **1980**, *102*, 6937.

JA964271E